• Basic Research •

Pyroptosis-associated inflammasome activation contributes to scleral remodeling in experimental myopia

Ai-Lin Wang[1], Qi Lyu[2], Hong-Mei Wang[3], Jing-Tian Zhang[4], Qin Long[1], Zhi-Kun Yang[1]

[1]Department of Ophthalmology, Peking Union Medical College Hospital, Chinese Academy of Medical Sciences and Peking Union Medical College, Beijing 100730, China
[2]Medical Science Academy, Shanxi Medical University, Taiyuan 030001, Shanxi Province, China
[3]Pingdingshan Second People's Hospital, Pingdingshan 467000, Henan Province, China
[4]Shenzhen Research Institute, Frontiers Science Center for Cell Responses, State Key Laboratory of Medicinal Chemical Biology, Key Laboratory of Bioactive Materials, Ministry of Education, College of Life Sciences, Nankai University, Tianjin 300071, China
Correspondence to: Qin Long and Zhi-Kun Yang. Department of Ophthalmology, Peking Union Medical College Hospital, Chinese Academy of Medical Sciences and Peking Union Medical College, Beijing 100730, China. longqinbj@hotmail.com; yangzhikun@pumch.cn
Received: 2026-01-21 Accepted: 2026-03-31

Abstract

● **AIM:** To explore whether pyroptosis, an inflammatory type of programmed cell death, participates in the initiation and progression of myopia, and to further elucidate its regulatory role in scleral remodeling.

● **METHODS:** Scleral tissues from form-deprivation myopia (FDM) mouse models were subjected to transcriptome sequencing to screen inflammatory and cell death-related molecular characteristics. Differentially expressed gene analysis and pathway enrichment analysis were adopted to identify pyroptosis-related signaling pathways. Meanwhile, human scleral fibroblasts were treated with complement component 3a (C3a) to construct an *in vitro* inflammatory cell model. Western blot, immunofluorescence staining, lactate dehydrogenase (LDH) release assay and transmission electron microscopy were applied to detect extracellular matrix (ECM) alterations and the expression levels of core pyroptosis markers including NOD-like receptor family pyrin domain-containing protein 3 (NLRP3), caspase-1 and N-terminal gasdermin D (GSDMD-N).

● **RESULTS:** Transcriptomic results revealed that inflammatory response, immune regulation, and pyroptosis-related pathways were significantly enriched in myopic scleral tissues, accompanied by synchronous activation of inflammasome signaling. *In vitro* inflammatory intervention downregulated the expression of type I collagen and upregulated matrix metalloproteinase-2 (MMP-2), suggesting aggravated ECM degradation. The levels of interleukin-1β (IL-1β), interleukin-18 (IL-18), cell membrane permeability, as well as NLRP3, caspase-1, and GSDMD-N were obviously increased in activated fibroblasts. Immunofluorescence and ultrastructural observations further confirmed gasdermin protein-mediated cell membrane damage and typical pyroptotic morphological changes.

● **CONCLUSION:** *In vivo* animal experiments and *in vitro* cellular studies collectively verify that the activation of inflammasome-caspase-1-GSDMD signaling axis is involved in myopia-related scleral remodeling. Pyroptosis acts as a key mechanistic bridge linking inflammatory response and scleral structural weakening, which offers novel molecular targets for the intervention and suppression of myopia progression.

● **KEYWORDS:** inflammasome; myopia; NLRP3; pyroptosis; scleral remodeling

DOI:10.18240/ijo.2026.07.04

Citation: Wang AL, Lyu Q, Wang HM, Zhang JT, Long Q, Yang ZK. Pyroptosis-associated inflammasome activation contributes to scleral remodeling in experimental myopia. *Int J Ophthalmol* 2026;19(7):1249-1258

INTRODUCTION

The frequency of myopia in young people and adolescents is steadily rising, making it a significant global public health concern[1-2]. The likelihood of blinding visual problems, like retinal detachment, myopic maculopathy, and glaucoma, is significantly increased by high myopia and may result in irreversible vision impairment[3-4]. Therefore, elucidating the molecular basis underlying myopia development and progression is essential for improving preventive strategies and identifying novel therapeutic targets.

Axial elongation is the principal structural hallmark of myopia, and scleral remodeling is widely regarded as the

key histological basis driving axial elongation[5]. Collagen fibers and proteoglycans are among the extracellular matrix (ECM) components that make up the sclera, which is essential for preserving the form and biomechanical stability of the eye[5-6]. Scleral fibroblasts are the major effector cells responsible for regulating ECM synthesis and degradation; their functional state directly influences collagen homeostasis and the expression of matrix remodeling enzymes[7-8]. Previous studies have shown that myopia progression is accompanied by dysregulated collagen metabolism, increased matrix metalloproteinase activity, and altered scleral biomechanical properties. However, the upstream cellular stress responses and molecular events that initiate these changes remain incompletely understood[9-10].

Usually taking place after inflammasome construction and activation, pyroptosis acts as a pro-inflammatory kind of programmed death of cells that depends on caspase stimulation. An essential intracellular pattern-identifying sensor, NOD-like receptor family pyrin domain-containing protein 3 (NLRP3), can detect a variety of microbial components, endogenous danger signals, and environmental stimuli, which encourages the development and activation of the NLRP3 inflammasome[11]. Inflammasome-triggered caspase-1 mediates the development and dissolution of interleukin (IL)-1β and IL-18 and breaks down gasdermin D (GSDMD) to generate an N-terminal fragment that creates holes in the plasma membrane, ultimately resulting in cell division and intensifying the inflammatory cascade[12].

Accumulating evidence indicates that chronic inflammation is closely associated with myopia progression[13-14]. Studies using form-deprivation myopia (FDM) models have suggested that scleral NLRP3 activation may participate in myopia development. NLRP3 pathway activation has been proposed to upregulate matrix metalloproteinase-2 (MMP-2) expression and influence collagen I metabolism, thereby contributing to scleral ECM remodeling and myopia progression[15]. Importantly, however, increased NLRP3 expression or activation reflects only a potential initiation of inflammasome-related signaling; the occurrence of pyroptosis requires complete inflammasome assembly, caspase-1 activation, and gasdermin-mediated membrane pore formation. Thus, NLRP3 upregulation does not necessarily equate to pyroptotic cell death. Given that myopia progression involves not only inflammatory responses but also structural remodeling of ocular tissues, pyroptosis, characterized by both inflammatory amplification and cell death, may be involved in translating inflammatory signaling into tissue injury and scleral remodeling. Accordingly, systematically investigating whether pyroptosis occurs in myopia and delineating its underlying mechanisms is of substantial theoretical significance and potential clinical value.

Based on this background, we hypothesized that the myopia-associated inflammatory microenvironment may trigger pyroptosis-related molecular events in the sclera and disrupt ECM metabolic homeostasis in scleral fibroblasts. To test this hypothesis, we established a mouse FDM model and performed transcriptomic profiling of scleral tissues, integrating differential expression and pathway enrichment analyses to characterize inflammatory and inflammasome-related signatures. Because complement-related inflammatory signaling emerged from prior myopia-related studies and C3a has been shown to affect scleral fibroblast biology, C3a-treated human scleral fibroblasts (HSFs) were used as an *in vitro* inflammatory model to validate transcriptome-derived mechanistic clues. In parallel, we treated scleral fibroblasts with the complement component C3a to establish an *in vitro* model and systematically evaluated ECM remodeling phenotypes and pyroptosis-related events using multi-dimensional molecular and functional assays.

MATERIALS AND METHODS

Ethical Approval All experimental procedures involving animals and human tissues were reviewed and approved by the Ethics Committee of Peking Union Medical College Hospital (Approval No. XHDW-2025-154). Animal experiments were conducted in accordance with the ARVO Statement for the Use of Animals in Ophthalmic and Vision Research. HSFs were obtained from donor scleral tissues provided by the Eye Bank of Beijing Tongren Hospital, and all procedures involving human tissues were performed in accordance with the Declaration of Helsinki.

Model of Form-Deprivation Myopia Three-week-old male C57BL/6J mice were obtained from Beijing Vital River Laboratory Animal Technology Co., Ltd. (Beijing, China). Mice were housed under standard laboratory conditions with a 12-hour light/12-hour dark cycle and had free access to food and water.

As previously mentioned, the model of FDM was created with a few minor adjustments[16]. Briefly, mice were randomly assigned to the form-deprivation group (n=20) or a normal control group (n=20). In the form-deprivation group, the right eye was covered with a handmade semi-transparent diffuser constructed from balloon material to induce form deprivation. The diffuser was secured around the periocular region, and a neck collar was fitted to prevent removal. The position and integrity of the diffuser were inspected daily to ensure continuous deprivation. Following four weeks of form deprivation, axial length and refractive status were assessed as follows.

Measurement of Axial Length and Refraction Before refraction assessment, mice were anesthetized with inhaled isoflurane until adequately sedated, and 1% tropicamide was

instilled for pupil dilation. A streak retinoscope (66 Vision Technology Co., Ltd., Suzhou, China) was used to test refraction in a dark room. After refraction assessment, mice were euthanized under deep isoflurane anesthesia. Eyes were immediately enucleated, and the surrounding connective tissues were carefully removed. A digital vernier caliper was used to measure axial length. Each eye was examined three times, and the mean value was used for further analysis.

Scleral Tissue Collection, RNA Extraction, and RNA Sequencing After completion of form deprivation, mice were euthanized, and the scleral tissues were carefully dissected under a stereomicroscope. Given the low RNA yield from scleral tissues, three scleral samples were pooled to generate one biological sample, and four biological replicates were prepared for each group. As directed by the manufacturer, total RNA was collected using TRIzol reagent. RNA concentration and purity were measured with a Thermo Fisher Scientific NanoDrop 2000 spectrophotometer, and RNA integrity was assessed using an Agilent 2100 Bioanalyzer (Agilent Technologies).

RNA-seq libraries were created using the NEBNext Ultra II RNA Library Prep Kit for Illumina (New England Biolabs). To summarize, oligo(dT) magnetic beads were employed to enrich poly(A)+mRNA, which was then broken down, subjected to first- and second-strand cDNA synthesis, final repair, A-tailing, adaptor ligation, and polymerase chain reaction (PCR) amplification. The library's quality was evaluated using the Agilent 2100 Bioanalyzer. Personal Biotechnology Co., Ltd. (China) performed the sequencing *via* paired-end 150 bp reads on an Illumina platform.

Analysis of Bioinformatics FASTQ-formatted raw sequencing data were acquired. Fastp (v0.22.0) for quality control and filtering to eliminate adaptor sequences and low-quality reads. A public database was used to obtain the mouse reference genome and related annotation files. HISAT2 (v2.1.0) was used to align clean reads to the reference genome. Gene-level read counts were generated using HTSeq (v0.9.1). Gene expression levels were normalized as fragments per kilobase of transcript per million mapped reads (FPKM) for expression visualization. DESeq2 was used to carry out differential expression analysis on raw read counts. Differentially expressed genes (DEGs) are classified as genes with $|\log_2(\text{fold change})|>1.5$ and $P<0.05$. R was used for principal component analysis (PCA), hierarchical clustering, and DEG visualization, including heatmaps and volcano plots. Gene Ontology (GO) enrichment analysis by means of a hypergeometric test was run using the topGO software; $P<0.05$ was regarded as statistically significant. Kyoto Encyclopedia of Genes and Genomes (KEGG) analysis of pathway enrichment was performed using the clusterProfiler application. Gene set enrichment analysis (GSEA) was executed by GSEA software (v4.1.0). The enrichment of predetermined gene sets throughout the ranking list was evaluated after all genes were ranked according to how differently they expressed themselves between groups.

Cell Culture and Establishment of an *in vitro* Myopia-Related Model HSFs were obtained from donor scleral tissues provided by the Eye Bank of Beijing Tongren Hospital. The donors had no prior experience of damage to the eyes or illness.

HSFs were raised in DMEM/F12 medium along with 15% fetal bovine serum and 1% penicillin-streptomycin. The cells were kept at 37℃ in an incubator that is humidified with 5% CO_2. Experiments were conducted using cells from passages 5 through 10.

Recombinant human complement component C3a (R&D Systems, 3677-C3) was applied to HSFs for 72h at a final dose of 0.1 μmol/L to create an *in vitro* myopia-related model. As a negative control, cells were cultured in culture media alone[17].

Cell Viability Assay Having been seeded into 96-well plates at a density of 5×10^3 cells/well, HSFs were cultured overnight to promote adhesion. After that, cells were exposed to 0.1 μmol/L recombinant human C3a for 72h, with untreated cells acting as controls. For every condition, there were five technical replicates. Cell viability was evaluated using a cell counting kit-8 (CCK-8) kit (Lablead Biotechnology, CK001) as directed by the manufacturer. In conclusion, 10 μL of CCK-8 solution was added to each well, and the combination was then incubated at 37℃ for 4h. A microplate reader was used to measure absorbance at 450 nm (Spark, Tecan, Austria).

Western Blotting Cells were lysed in RIPA buffer supplemented with protease and phosphatase inhibitors. Lysates were centrifuged at 4℃, and supernatants were collected. Protein concentrations were measured employing a bicinchoninic acid (BCA) protein assay kit (Beyotime Biotechnology, China). Equal amounts of protein were separated utilizing sodium dodecyl sulfate-polyacrylamide gel electrophoresis (SDS-PAGE) and then transferred to polyvinylidene difluoride (PVDF) membranes.

The membranes were covered with 5% non-fat milk at room temperature, and subsequently, they were incubated with primary antibodies for an entire night at 4℃. NLRP3 (Cell Signaling Technology, 15101T), caspase-1 (Proteintech, 22915-1-AP), IL-1β (Cell Signaling Technology, 12242T), IL-18 (Proteintech, 10663-1-AP), GSDMD-N (Abcam, ab215203), MMP-2 (Proteintech, 10373-2-AP), collagen I (Proteintech, 14695-1-AP), and glyceraldehyde-3-phosphate dehydrogenase (GAPDH; Proteintech, 60004-1-Ig) as loading controls. After being cleaned, membranes were then treated with either horseradish peroxidase (HRP)-conjugated goat

anti-rabbit immunoglobulin G (IgG; H+L; ABclonal, AS014) or HRP-conjugated goat anti-mouse IgG (H+L; ZSGB-BIO, Beijing, China; Cat. No. ZB-2305) for an hour at room temperature. Enhanced chemiluminescence (ECL) was used to visualize protein bands.

Immunofluorescence Staining Bovine serum albumin (BSA) was used to block the HSFs, followed by 20min of permeabilization with 0.5% Triton X-100 and 20min of fixation with 4% paraformaldehyde. An anti-GSDMD-N primary antibody (Abcam, ab215203) was used to incubate the cells for a whole night at 4℃. Following washing, after washing, cells were subjected to goat anti-rabbit IgG (H+L) secondary antibody marked with Alexa Fluor® 488 (Abcam, ab150077) for one hour at room temperature in the dark. Nuclei was counterstained using 4',6-diamidino-2-phenylindole (DAPI; Beyotime Biotechnology, C1006). Fluorescence images were acquired with a confocal laser scanning microscope, which ImageJ was then used to analyze.

Transmission Electron Microscopy The cells underwent dehydration, resin embedding, and polymerization after being fixed in 2.5% glutaraldehyde. To evaluate ultrastructural alterations, ultrathin sections (70–90 nm) were prepared, stained, and examined under a transmission electron microscope (TEM). Quantitative analysis of TEM images was performed to evaluate pyroptosis-related ultrastructural changes. Four representative non-overlapping TEM fields were randomly selected and analyzed for each group. Cells exhibiting at least two of the following morphological features were classified as pyroptosis-like cells: cytoplasmic vacuolization, cytoplasmic rarefaction, cell swelling, and plasma membrane rupture. The proportion of pyroptosis-like cells was calculated. In addition, the number of cytoplasmic vacuole-like structures per cell was quantified using ImageJ software.

Lactate Dehydrogenase Release To evaluate the integrity of the plasma membrane, LDH release in culture supernatants was measured using an LDH cytotoxicity test kit (Beyotime Biotechnology, C0016). The assay was performed according to the manufacturer's instructions. Absorbance was measured at 490 nm using a microplate reader, and LDH release levels were calculated based on absorbance values.

Statistical Analysis All quantitative data, including TEM-based ultrastructural analyses, are presented as mean±standard deviation (SD). Statistical analyses were carried out using GraphPad Prism (version 9.5.1). Two groups were compared using a two-tailed Student's *t*-test. $P<0.05$ was considered statistically significant.

RESULTS

Establishment of Myopia Models *in vivo* The form-deprivation group's eyes had significant myopia-related alterations in comparison to the normal control group's eyes. Refraction measurements showed a marked myopic shift in the experimental eyes (Figure 1A). Consistently, axial length analysis revealed a significant elongation of the eyeball in form-deprived eyes relative to controls (Figure 1B).

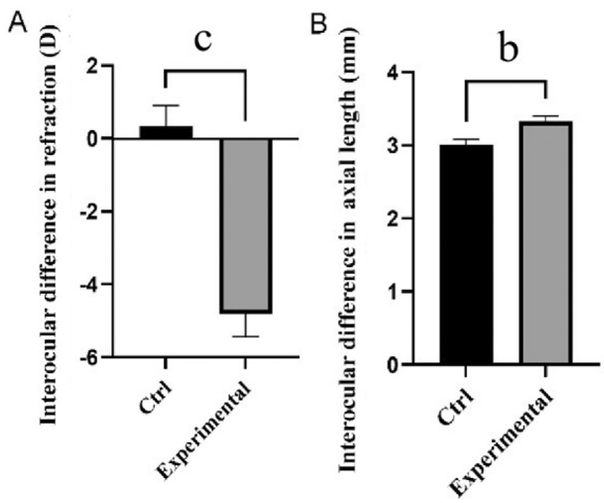

Figure 1 Establishment and validation of the form-deprivation myopia (FDM) mouse model A: Interocular differences in refractive error between control group and form-deprived eyes; B: Interocular differences in axial length between control group and form-deprived eyes. Data are presented as mean±SD. $^{b}P<0.01$, $^{c}P<0.001$. SD: Standard deviation.

Transcriptomic Analysis Revealed Inflammatory and Immune Activation in Myopic Sclera RNA sequencing was carried out on scleral tissues from experimental group and control group mice in order to examine molecular changes linked to experimental myopia. PCA effectively divided the experimental group and control group samples based on global gene expression profiles; PC1 and PC2 accounted for 69.8% and 14.8% of the total variance, respectively (Figure 2A), indicating significant transcriptome differences between the two groups.

Differential expression analysis identified 1251 DEGs, of which 1072 were significantly downregulated, and 179 were upregulated in the experimental group relative to the controls (Figure 2B). The location of DEGs was further demonstrated by the volcano plot, which showed a prominent downregulation pattern in the sclera after experimental myopia induction (Figure 2C).

Hierarchical clustering analysis based on DEGs showed high consistency among biological replicates and a clear segregation between the experimental group and control group samples (Figure 2D), supporting the robustness and reliability of the transcriptomic data. Collectively, these findings indicate that experimental myopia induces marked transcriptional reprogramming in mouse scleral tissue, characterized predominantly by widespread gene downregulation.

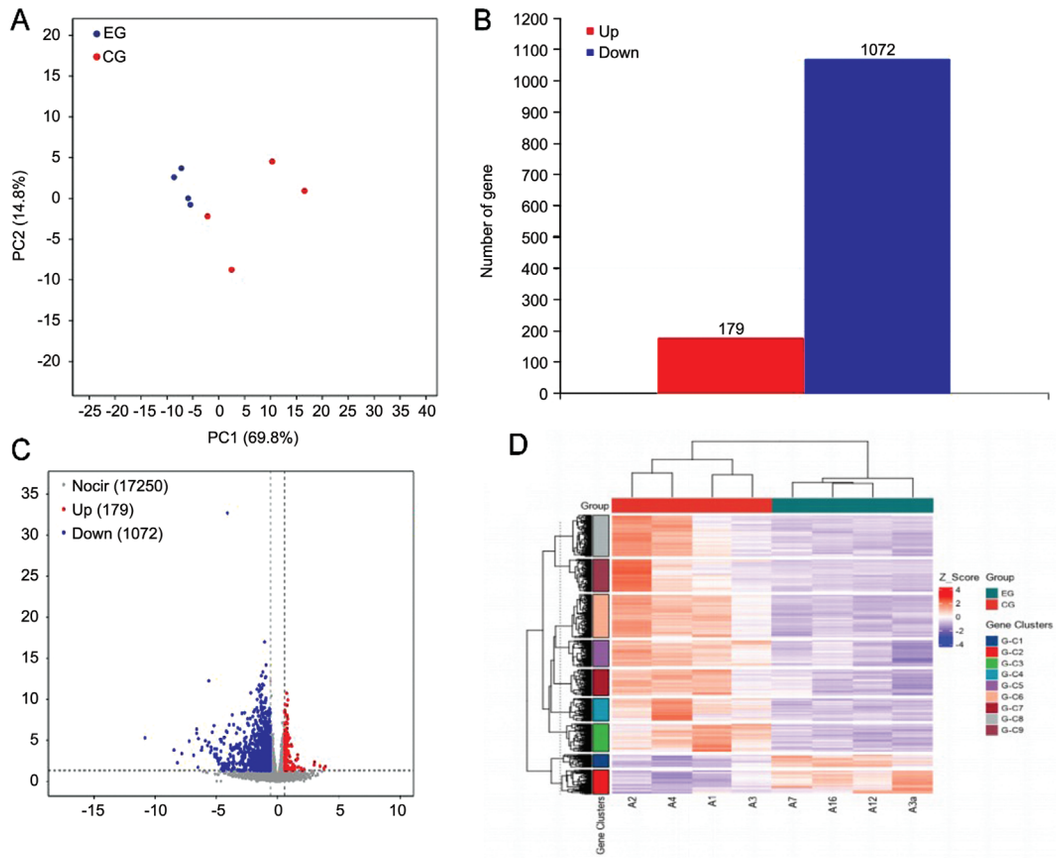

Figure 2 Transcriptomic profiling reveals marked transcriptional reprogramming in myopic sclera A: Principal component analysis (PCA) of scleral transcriptomes from experimental myopia (EG) and control (CG) groups; B: Bar plot showing the numbers of upregulated and downregulated differentially expressed genes (DEGs); C: Volcano plot illustrating the distribution of DEGs, with upregulated and downregulated genes indicated; D: Heatmap of hierarchical clustering based on DEGs between EG and CG groups.

Functional Enrichment Analysis Revealed Prominent Enrichment of Immune- and Inflammation-Related Pathways in Myopic Sclera The biological functions associated with the DEGs were further described using GO and KEGG pathway enrichment analysis. GO enrichment analysis revealed that DEGs were most abundant in immune-related biological processes, including immune system function, immunological response, defensive reaction, and inflammatory response. In addition, several cellular component categories, such as extracellular region and extracellular space, were also significantly enriched (Figure 3A). DEGs were substantially enriched in a number of immunological and cytokine-related signaling pathways, including complement and coagulation cascades, cytokine-cytokine receptor interaction, tumor necrosis factor (TNF), nuclear factor (NF)-κB, JAK-STAT, and IL-17 signaling pathways, according to KEGG pathway analysis (Figure 3B).

Based on ranking gene lists, GSEA (Figure 3C) further demonstrated coordinated transcriptional changes, with several pathways linked to inflammation and the immune system exhibiting notable enrichment in the myopia model.

Collectively, these findings indicate that experimental myopia is accompanied by pronounced enrichment of immune- and inflammation-related molecular signatures in scleral tissues, providing a rationale for further investigation of inflammation-associated mechanisms.

Establishment of Myopia Models *in vitro* The viability of the *in vitro* myopia-related cellular model was assessed using a CCK-8 assay to evaluate overall cellular metabolic activity. This assay was primarily performed to confirm that C3a stimulation did not induce nonspecific cytotoxicity and that the experimental condition was suitable for modeling a myopia-related inflammatory microenvironment. When contrasted with the control group, the C3a treatment resulted in a slight but statistically significant reduction in cell viability, as seen in Figure 4A, suggesting that overall metabolic activity remained largely preserved under the experimental conditions rather than indicating extensive nonspecific cytotoxicity. It should be noted that the CCK-8 assay primarily reflects cellular metabolic activity and does not distinguish specific modes of cell death. Therefore, additional molecular, membrane-permeability, and ultrastructural analyses were performed to evaluate pyroptosis-associated cellular injury.

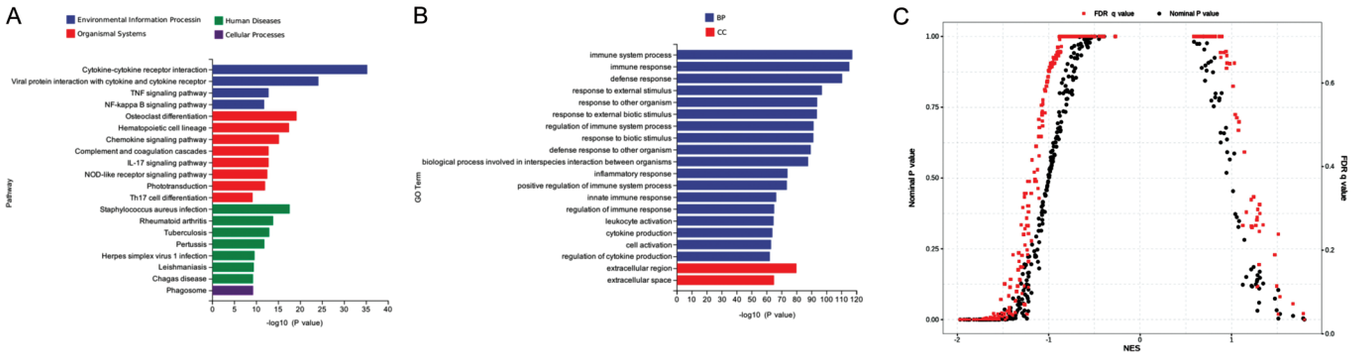

Figure 3 Functional enrichment analyses identify inflammation- and cell death-related molecular signatures in myopic sclera A: Kyoto Encyclopedia of Genes and Genomes (KEGG) pathway enrichment analysis of differentially expressed genes (DEGs); B: Gene Ontology (GO) enrichment analysis; C: Gene set enrichment analysis (GSEA). NES: Normalized enrichment score; FDR: False discovery rate.

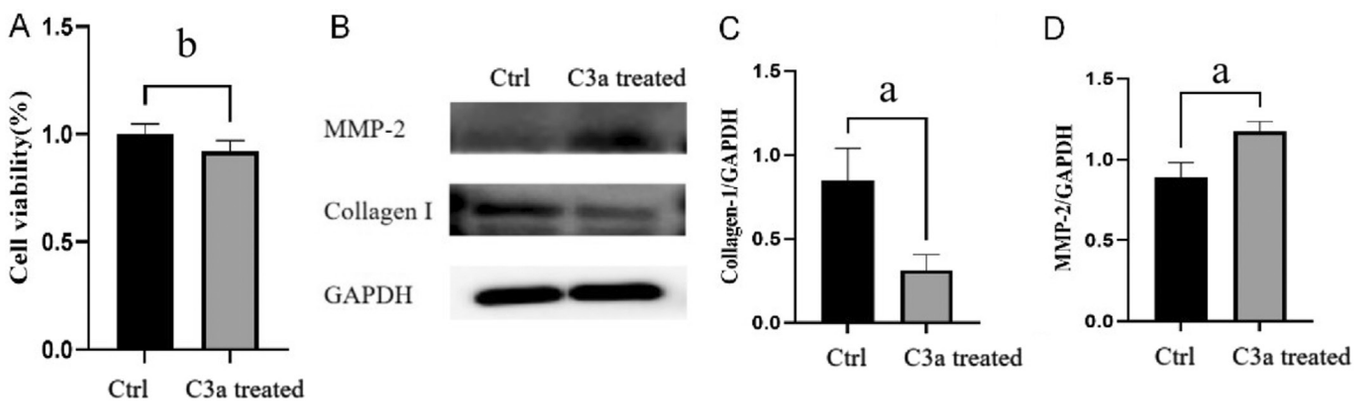

Figure 4 Inflammatory stimulation induces extracellular matrix remodeling in scleral fibroblasts A: CCK-8 assay showing overall metabolic activity of scleral fibroblasts following C3a treatment; B: Representative Western blot images showing collagen I and MMP-2 expression in control and C3a-treated scleral fibroblasts; C: Quantitative analysis of collagen I protein levels normalized to GAPDH; D: Quantitative analysis of MMP-2 protein levels normalized to GAPDH. Data are presented as mean±SD. [a]*P*<0.05, [b]*P*<0.01. MMP: Matrix metalloproteinase-2; GAPDH: Glyceraldehyde-3-phosphate dehydrogenase; CCK: Cell counting kit; SD: Standard deviation.

In addition, collagen I expression decreased while MMP-2 expression increased in C3a-treated scleral fibroblasts, suggesting a shift toward ECM degradation (Figure 4B–4D).

Collectively, these results demonstrate robust myopia-related changes *in vivo* and confirm the suitability of C3a treatment for subsequent *in vitro* mechanistic investigations.

Pyroptosis-Related Molecular Signatures in Scleral Fibroblasts Under Experimental Conditions Given that transcriptomic analyses revealed prominent enrichment of immune- and inflammation-related pathways in myopic sclera, we next examined pyroptosis-related molecules and ECM remodeling-associated proteins in scleral fibroblasts under experimental treatment conditions.

Western blot analysis showed increased expression of NLRP3, caspase-1, and GSDMD-N in C3a-treated cells compared with controls (Figure 5A–5D).

The treated group consistently had greater protein levels of the cytokines that promote inflammation, IL-1β, and IL-18, suggesting an improved inflammation-related molecular response (Figure 5E–5F). Furthermore, the C3a-treated group showed a substantial increase in LDH release, which suggests greater membrane permeability and cellular injury (Figure 5G).

Collectively, these findings indicate activation of the NLRP3 inflammasome and the downstream caspase-1-GSDMD signaling axis, which is commonly associated with canonical pyroptosis.

Pyroptosis-Related Morphological Changes and Membrane Damage in C3a-Treated Scleral Fibroblasts To further validate pyroptosis-associated cellular injury at the ultrastructural level, TEM analysis was performed. Based on the observed upregulation of pyroptosis-related molecular markers, we next examined morphological and functional alterations in scleral fibroblasts using immunofluorescence staining, ultrastructural analysis, and membrane integrity assays. Immunofluorescence analysis revealed a markedly increased GSDMD-N signal in C3a-treated cells compared with controls. While control cells only showed mild basal expression, GSDMD-N fluorescence was primarily seen in the cytoplasm and along the plasma membrane, suggesting increased pyroptosis-associated signaling at the cellular

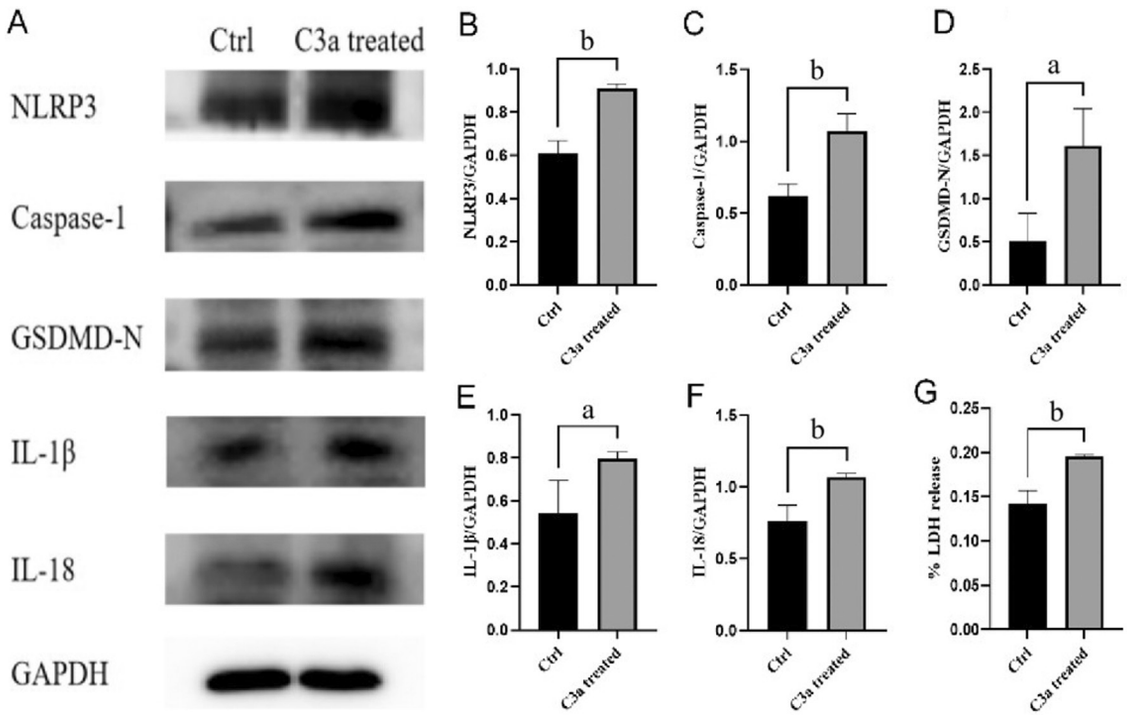

Figure 5 Activation of the inflammasome-caspase-1-GSDMD axis and increased membrane permeability in scleral fibroblasts A: Representative Western blot images showing expression of NLRP3, caspase-1, cleaved gasdermin D (GSDMD-N), IL-1β, and IL-18 in control and C3a-treated scleral fibroblasts; B–D: Quantitative of NLRP3, caspase-1, GSDMD-N; E, F: Quantitative analysis of IL-1β and IL-18 protein levels normalized to GAPDH; G: LDH release assay showing increased membrane permeability in C3a-treated cells. Data are presented as mean±SD. [a]*P*<0.05, [b]*P*<0.01. NLRP3: NOD-like receptor protein 3; GSDMD-N: Cleaved gasdermin D; IL-1β: Interleukin-1β; IL-18: Interleukin-18; GAPDH: Glyceraldehyde-3-phosphate dehydrogenase; LDH: Lactate dehydrogenase; SD: Standard deviation.

level (Figure 6A). Consistently, TEM revealed pronounced ultrastructural alterations in C3a-treated cells. These changes included disrupted plasma membrane integrity (black arrows), increased vacuole-like structures within the cytoplasm (white arrows), and overall cytoplasmic rarefaction, which are consistent with morphological features associated with pyroptosis (Figure 6B). Quantitative analysis of representative TEM fields further showed that the proportion of pyroptosis-like cells was significantly higher in the treated group than in the control group (Figure 6C). In addition, the number of cytoplasmic vacuole-like structures per cell was significantly increased in C3a-treated cells (Figure 6D). Collectively, these findings provide both morphological and quantitative evidence that C3a treatment induces pyroptosis-related cellular alterations in scleral fibroblasts, supporting a potential role of inflammasome-mediated cell injury in myopia-associated scleral remodeling.

DISCUSSION

In this study, we combined scleral transcriptomic profiling with *in vitro* cell-based assays to investigate potential molecular mechanisms of inflammatory cell death in myopia-relevant tissues and cells. Transcriptomic analysis revealed significant enrichment of multiple pathways associated with inflammation, immune regulation, and programmed cell death in the sclera of experimental myopia. Complementary *in vitro* experiments further verified activation of the implicated pathways at the molecular, functional, and ultrastructural levels. Together, these tissue- and cell-level findings provide convergent evidence supporting the hypothesis that pyroptosis may be involved in myopia development and progression, and suggest that inflammatory cell death may be closely linked to myopia-associated scleral remodeling. To the best of our knowledge, studies specifically investigating pyroptosis-associated mechanisms in scleral fibroblasts during myopia progression remain limited, particularly in the context of scleral remodeling. The present findings provide additional evidence suggesting that inflammasome-mediated pyroptosis may be involved in myopia-associated scleral remodeling.

At the tissue level, scleral transcriptomic profiling indicated marked transcriptional reprogramming in experimental myopia, characterized by substantial alterations involving genes related to immune regulation and inflammatory responses[18-20]. DEGs were primarily found in pathways linked to inflammation, cellular stress responses, and programmed cell death, according to the KEGG, GO, and GSEA. Significantly, signaling pathways linked to inflammation and inflammasomes showed a coordinated enrichment pattern. This sustained inflammatory transcriptional profile may provide a molecular

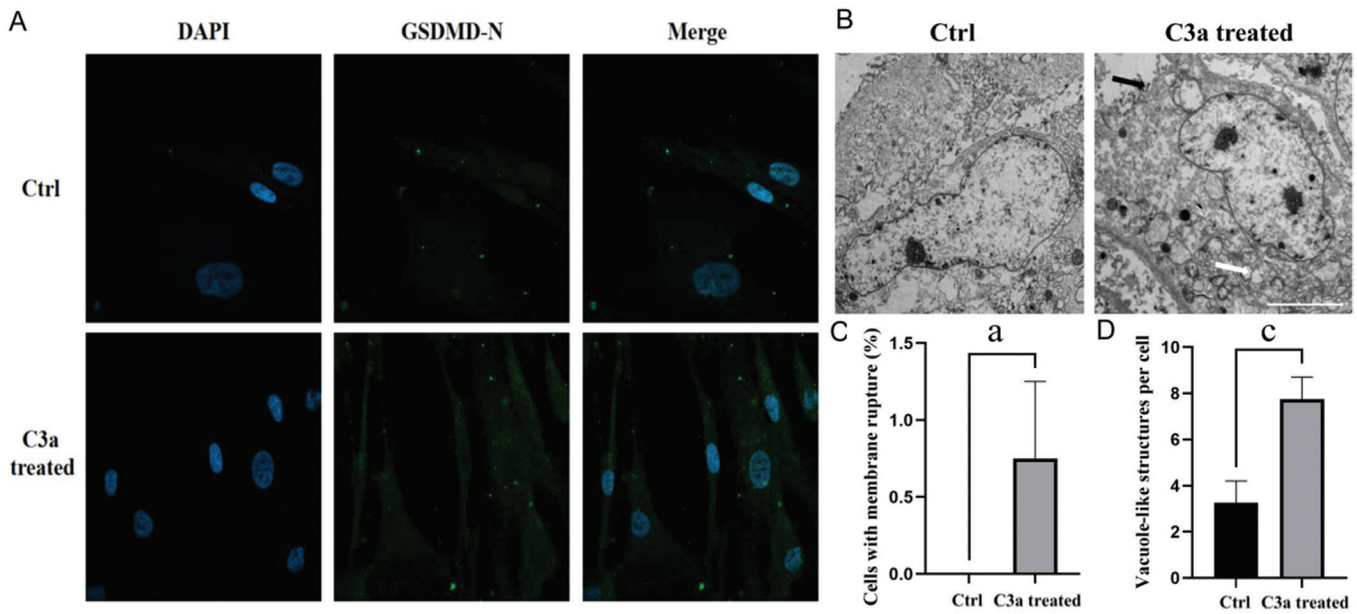

Figure 6 Pyroptosis-like morphological features and quantitative ultrastructural analysis in scleral fibroblasts A: Immunofluorescence staining showing GSDMD-N expression and subcellular localization in control and C3a-treated scleral fibroblasts. Nuclei were counterstained with DAPI. B: Representative transmission electron microscopy (TEM) images showing ultrastructural features consistent with pyroptosis-like cell injury, including disrupted plasma membrane integrity (black arrows) and increased cytoplasmic vacuole-like structures (white arrows). C: Quantitative analysis of pyroptosis-like cells in representative TEM fields. D: Quantification of cytoplasmic vacuole-like structures per cell. *n*=4 fields. Data are presented as mean±SD. $^{a}P<0.05$, $^{c}P<0.001$. Scale bars=5 μm. GSDMD-N: N-terminal gasdermin D. DAPI: 4′,6-diamidino-2-phenylindole; SD: Standard deviation.

context conducive to inflammation-associated cellular state changes and inflammatory cell death, and it offered key clues guiding subsequent validation of pyroptosis-related events at the protein and functional levels.

We created an *in vitro* myopia-related model employing scleral fibroblasts in order to evaluate the molecular characteristics indicated by the transcriptome data in a pertinent cellular setting. Under inflammatory stimulation, cell viability showed a mild but statistically significant decrease without obvious nonspecific cytotoxicity. The relatively preserved CCK-8 signal does not exclude pyroptosis-associated injury, because this assay primarily reflects metabolic activity rather than specific cell death modalities. In inflammatory microenvironments, pyroptosis may occur in a subset of cells without causing extensive loss of overall cell viability. Concurrently, collagen I was downregulated and MMP-2 was upregulated, indicating a shift in ECM metabolic balance toward degradation-consistent with molecular features of myopia-associated scleral remodeling[21-22]. Building on these observations, we further assessed inflammatory cell death-related events. Treated cells exhibited significantly increased membrane permeability, accompanied by upregulation of key inflammasome pathway components, including NLRP3, caspase-1, and the cleaved form of GSDMD-N, as well as increased levels of IL-1β and IL-18. Immunofluorescence further demonstrated enhanced GSDMD-N signals with altered subcellular distribution, while TEM revealed cellular swelling and compromised plasma membrane integrity. Collectively, these functional, molecular, and morphological findings support activation of the inflammasome-caspase-1-GSDMD axis in scleral fibroblasts, providing direct experimental evidence for pyroptosis-associated molecular events and corroborating the transcriptomic signatures observed in myopic sclera.

Accumulating evidence has indicated that inflammatory responses play an important role in myopia progression. Previous studies by several groups demonstrated upregulation of multiple inflammation-related factors, such as NF-κB and IL-6, in FDM models, while anti-inflammatory interventions could partially attenuate myopia progression[23-26]. In addition, the immunosuppressant cyclosporin A has been reported to suppress myopia development, further supporting a role of inflammation in myopia pathogenesis[22]. Within inflammatory signaling networks, the NLRP3 inflammasome is a key regulatory node controlling the maturation of pro-inflammatory cytokines. According to earlier research, NLRP3 activation stimulates caspase-1 activation and the release of IL-1β. IL-1β can influence ECM degradation and tissue remodeling by modulating MMP-2 levels through a variety of routes[27-29].

Importantly, NLRP3 inflammasome activation not only regulates inflammatory cytokine production but also represents a critical upstream event in inflammatory cell death. By encouraging the release of IL-1β and IL-18 upon

inflammasome assembly, activated caspase-1 increases inflammatory responses. At the same time, it cleaves gasdermin proteins to cause membrane pore development and lysis of cells, demonstrating the simultaneous existence of inflammatory amplification and the execution of programmed cell death[30-33]. Based on these findings, we propose that NLRP3 may contribute to myopia-associated scleral remodeling through at least two complementary routes: 1) by regulating ECM metabolism *via* an inflammatory cytokine-MMP axis; 2) by inducing pyroptosis in scleral fibroblasts, thereby impairing cellular function and homeostatic maintenance of the ECM. In this framework, NLRP3-driven signaling may serve as a mechanistic bridge linking myopia-related inflammation to structural alterations of the sclera.

Scleral fibroblasts play a central role in maintaining scleral ECM homeostasis and biomechanical stability. These cells are responsible for the synthesis and turnover of major ECM components, including collagen type I, collagen type III, and proteoglycans. If pyroptosis occurs in scleral fibroblasts, the loss of viable fibroblasts may reduce ECM synthesis capacity and disrupt the balance between ECM production and degradation. In addition, pyroptosis is accompanied by the release of pro-inflammatory cytokines, which may further stimulate matrix-degrading enzymes such as MMPs and accelerate ECM breakdown. The combined effects of reduced collagen synthesis and enhanced ECM degradation may lead to scleral thinning and decreased biomechanical strength. Such structural weakening of the sclera is considered an important factor contributing to scleral remodeling and axial elongation during myopia development. Therefore, pyroptosis-induced injury to scleral fibroblasts may represent a potential mechanism linking inflammation to scleral remodeling in myopia.

This study has some sort of limitations that should be mentioned. First, although the transcriptomic and *in vitro* data collectively support the presence of pyroptosis-related molecular events and the involvement of the inflammasome-caspase-1-GSDMD axis in a myopia-associated inflammatory microenvironment, we did not directly test causality through *in vivo* targeted intervention of key pathway components. Future studies should combine pharmacological inhibitors and genetic approaches to modulate inflammasome or pyroptosis key nodes in myopia models and evaluate their effects on scleral remodeling phenotypes and refractive outcomes, thereby clarifying the functional contribution of this pathway to myopia development and progression.

Second, while the *in vitro* scleral fibroblast model provides important mechanistic clues, myopia is a multifactorial and complex disease process. The upstream triggers of local inflammasome activation in the sclera and the cell-type specificity of pyroptosis-related events remain to be elucidated. Future work should dissect the sources and regulatory networks of these signals at finer cellular and tissue resolution, ideally integrating *in vivo* functional validation, to further refine the mechanistic framework of scleral remodeling in myopia.

In summary, by integrating unbiased transcriptomic profiling with *in vivo* and *in vitro* experimental validation, this study reveals coordinated alterations in immune- and inflammation-related molecular networks in the sclera during experimental myopia. In a scleral fibroblast-based model, we further observed ECM remodeling features alongside inflammasome-caspase-1-GSDMD axis-associated molecular events and increased membrane permeabilization. Together, these converging lines of evidence suggest that pyroptosis-associated events may be engaged within the myopia-related inflammatory microenvironment, particularly at the level of scleral fibroblasts, and that inflammation-associated cell death processes in scleral fibroblasts may contribute to scleral remodeling and axial elongation.

Our findings offer further mechanistic insight into the relationship between inflammation and structural remodeling in myopia and suggest that pyroptosis-associated pathways may represent potential targets for future therapeutic exploration, even though *in vivo* functional interventions are necessary to establish causality.

ACKNOWLEDGEMENTS

Foundation: Supported by Beijing Natural Science Foundation (No.7252105).

Conflicts of Interest: Wang AL, None; **Lyu Q,** None; **Wang HM,** None; **Zhang JT,** None; **Long Q,** None; **Yang ZK,** None.

REFERENCES

1 Shinojima A, Negishi K, Tsubota K, *et al*. Multiple factors causing myopia and the possible treatments: a mini review. *Front Public Health* 2022;10:897600.

2 Liang JH, Pu YQ, Chen JQ, *et al*. Global prevalence, trend and projection of myopia in children and adolescents from 1990 to 2050: a comprehensive systematic review and meta-analysis. *Br J Ophthalmol* 2025;109(3):362-371.

3 Du Y, Meng JQ, He WW, *et al*. Complications of high myopia: an update from clinical manifestations to underlying mechanisms. *Adv Ophthalmol Pract Res* 2024;4(3):156-163.

4 Xia YT, Ge JY, Zhang ZC, *et al*. Macular epiretinal membrane in high myopia: timing and prognosis of pars plana vitrectomy surgery. *Int J Ophthalmol* 2025;18(9):1689-1696.

5 Brown DM, Kowalski MA, Paulus QM, *et al*. Altered structure and function of murine sclera in form-deprivation myopia. *Invest Ophthalmol Vis Sci* 2022;63(13):13.

6 Yasir ZH, Sharma R, Zakir SM. Scleral collagen cross linkage in progressive myopia. *Indian J Ophthalmol* 2024;72(2):174-180.

7 Summers Rada JA, Shelton S, Norton TT. The sclera and myopia. *Exp Eye Res* 2006;82(2):185-200.

8 Zhu CC, Chen QZ, Yuan Y, *et al*. Endoplasmic reticulum stress regulates scleral remodeling in a guinea pig model of form-deprivation myopia. *J Ophthalmol* 2020;2020(1):3264525.

9 Zhao F, Zhou QY, Reinach PS, *et al*. Cause and effect relationship between changes in scleral matrix metallopeptidase-2 expression and myopia development in mice. *Am J Pathol* 2018;188(8):1754-1767.

10 Yin XF, Ge JL. The role of scleral changes in the progression of myopia: a review and future directions. *Clin Ophthalmol* 2026;19:1699-1707.

11 Swanson KV, Deng M, Ting JP. The NLRP3 inflammasome: molecular activation and regulation to therapeutics. *Nat Rev Immunol* 2019;19(8):477-489.

12 Man SM, Karki R, Kanneganti TD. Molecular mechanisms and functions of pyroptosis, inflammatory caspases and inflammasomes in infectious diseases. *Immunol Rev* 2017;277(1):61-75.

13 Chou YL, Hsu YA, Lin CF, *et al*. Complement decay-accelerating factor inhibits inflammation-induced myopia development. *Mol Immunol* 2024;171:47-55.

14 Chen KW, Broz P. Gasdermins as evolutionarily conserved executors of inflammation and cell death. *Nat Cell Biol* 2024;26(9):1394-1406.

15 Chen ZY, Xiao K, Long Q. Up-regulation of NLRP3 in the sclera correlates with myopia progression in a form-deprivation myopia mouse model. *Front Biosci* (*Landmark Ed*) 2023;28(2):27.

16 Xiao K, Chen ZY, He SQ, *et al*. Up-regulation of scleral C5b-9 and its regulation of the NLRP3 inflammasome in a form-deprivation myopia mouse model. *Immunobiology* 2024;229(1):152776.

17 Xiao K, Jie Y, Luo MY, *et al*. Cytological and functional effect of complement 3a on Human Scleral Fibroblasts. *Cutan Ocul Toxicol* 2023;42(3):137-143.

18 Kim H, Lee W, Kim YA, *et al*. RNA-sequencing analysis reveals the role of mitochondrial energy metabolism alterations and immune cell activation in form-deprivation and lens-induced myopia in mice. *Genes (Basel)* 2023;14(12):2163.

19 Zhao LH, Zhou Y, Jiang ZY, *et al*. Selenide-modified hyaluronic acid hydrogel promotes scleral remodeling during the recovery phase of form-deprivation myopia by inhibiting HIF-1α-mediated inflammation. *Int J Biol Macromol* 2025;311:143385.

20 Zeng L, Li XN, Liu J, *et al*. RNA-seq analysis reveals an essential role of the tyrosine metabolic pathway and inflammation in myopia-induced retinal degeneration in guinea pigs. *Int J Mol Sci* 2021;22(22):12598.

21 Gentle A, Liu YY, Martin JE, *et al*. Collagen gene expression and the altered accumulation of scleral collagen during the development of high myopia. *J Biol Chem* 2003;278(19):16587-16594.

22 McBrien NA, Jobling AI, Gentle A. Biomechanics of the sclera in myopia: extracellular and cellular factors. *Optom Vis Sci* 2009;86(1):E23-E30.

23 Hsu YA, Chen CS, Wang YC, *et al*. Anti-inflammatory effects of resveratrol on human retinal pigment cells and a myopia animal model. *Curr Issues Mol Biol* 2021;43(2):716-727.

24 Jiang LQ, Koh JHZ, Seah SHY, *et al*. Key role for inflammation-related signaling in the pathogenesis of myopia based on evidence from proteomics analysis. *Sci Rep* 2024;14:23486.

25 Zhang J, Kamoi K, Zong Y, *et al*. Inflammation and immune pathways in myopia: an overview on pathomechanisms and treatment prospects. *Clin Rev Allergy Immunol* 2025;68(1):98.

26 Xu R, Zheng J, Liu LQ, *et al*. Effects of inflammation on myopia: evidence and potential mechanisms. *Front Immunol* 2023;14:1260592.

27 Dai JZ, Shen JJ, Chai YM, *et al*. IL-1β impaired diabetic wound healing by regulating MMP-2 and MMP-9 through the p38 pathway. *Mediat Inflamm* 2021;2021(1):6645766.

28 Wang CL, Chi QJ, Sha YQ, *et al*. Mechanical injury and IL-1β regulated LOXs and MMP-1, 2, 3 expression in ACL fibroblasts co-cultured with synoviocytes. *Biotechnol Lett* 2020;42(8):1567-1579.

29 Kimura K, Zhou HY, Orita T, *et al*. Suppression by an RAR-γ agonist of collagen degradation mediated by corneal fibroblasts. *Invest Ophthalmol Vis Sci* 2017;58(4):2250.

30 Strowig T, Henao-Mejia J, Elinav E, *et al*. Inflammasomes in health and disease. *Nature* 2012;481(7381):278-286.

31 Hu JJ, Liu X, Xia SY, *et al*. FDA-approved disulfiram inhibits pyroptosis by blocking gasdermin D pore formation. *Nat Immunol* 2020;21(7):736-745.

32 Wang YP, Gao WQ, Shi XY, *et al*. Chemotherapy drugs induce pyroptosis through caspase-3 cleavage of a gasdermin. *Nature* 2017;547(7661):99-103.

33 Fu JN, Wu H. Structural mechanisms of NLRP3 inflammasome assembly and activation. *Annu Rev Immunol* 2023;41:301-316.